

Nature of the anomalies in the supercooled liquid state of the mW model of water

Vincent Holten,¹ David T. Limmer,² Valeria Molinero,³ and Mikhail A. Anisimov^{1, a)}

¹*Institute for Physical Science and Technology and Department of Chemical and Biomolecular Engineering, University of Maryland, College Park, Maryland 20742, USA*

²*Department of Chemistry, University of California, Berkeley, California 94720, USA*

³*Department of Chemistry, University of Utah, Salt Lake City, Utah 84112-0580, USA*

(Dated: 4 June 2018)

The thermodynamic properties of the supercooled liquid state of the mW model of water show anomalous behavior. Like in real water, the heat capacity and compressibility sharply increase upon supercooling. One of the possible explanations of these anomalies, the existence of a second (liquid–liquid) critical point, is not supported by simulations for this model. In this work, we reproduce the anomalies of the mW model with two thermodynamic scenarios: one based on a non-ideal “mixture” with two different types of local order of the water molecules, and one based on weak crystallization theory. We show that both descriptions accurately reproduce the model’s basic thermodynamic properties. However, the coupling constant required for the power laws implied by weak crystallization theory is too large relative to the regular backgrounds, contradicting assumptions of weak crystallization theory. Fluctuation corrections outside the scope of this work would be necessary to fit the forms predicted by weak crystallization theory. For the two-state approach, the direct computation of the low-density fraction of molecules in the mW model is in agreement with the prediction of the phenomenological equation of state. The non-ideality of the “mixture” of the two states never becomes strong enough to cause liquid–liquid phase separation, also in agreement with simulation results.

I. INTRODUCTION

The peculiar properties of supercooled water continue to gain interest. In the supercooled region, the thermodynamic response functions, namely heat capacity,¹ thermal expansivity,^{2,3} and compressibility,⁴ show strong temperature dependences suggesting a possible divergence at a temperature just below the homogeneous ice nucleation limit. One of the scenarios to explain the anomalous behavior of real water is the existence of a liquid–liquid transition terminated by the liquid–liquid critical point.^{5–14} An explicit equation of state based on this scenario is able to accurately represent all experimental data on the thermodynamic properties of supercooled water.¹⁵ If it exists, the second critical point of water cannot be directly observed in a bulk experiment, because it is located in “no man’s land,” below the homogeneous ice nucleation temperature.^{16,17} Computer simulations of water can provide additional insights into the nature of water’s anomalies. The mW model devised by Molinero and Moore¹⁸ represents the water molecule as a single atom with only short-range interactions, and is suitable for fast computations. The mW model imitates the anomalous behavior of cold and supercooled water, including the density maximum and the increase of the heat capacity and compressibility in the supercooled region.^{18–20} Using molecular dynamics simulations, Limmer and Chandler²⁰ have shown that the mW model does not exhibit a second critical point or liquid–liquid separation in the

range studied (0 MPa to 290 MPa, down to 170 K). Indeed, Moore and Molinero¹⁹ have demonstrated that in this model the supercooled liquid can no longer be equilibrated before it crystallizes and there is no sign of a liquid–liquid transition at supercooling. This raises the question: what is the origin of the anomalies in the mW model? In this work, we explain and reproduce these anomalies with a thermodynamic equation of state based on a non-ideal “mixture” of two kinds of molecular environments, in which the non-ideality is mainly entropy driven. By analyzing experimental data with this equation of state, Anisimov and coworkers^{15,21} have concluded that a liquid–liquid transition can occur if effects of crystallization are neglected. We show that for the mW model the nonideality of the free energy of mixing never becomes large enough to cause liquid–liquid phase separation. Finally, we show that the properties of the mW model may be described by power laws suggested by weak crystallization theory, which predicts apparently diverging corrections to the regular thermodynamic properties as a result of fluctuations in the translational order parameter, close to the limit of stability of the liquid phase. However, the resulting value of the coupling constant is large, which contradicts the basic assumption of the theory that the corrections must always remain smaller than the regular backgrounds, suggesting that fluctuation corrections beyond what are considered here may be important.

II. TWO-STATE THERMODYNAMICS OF LIQUID WATER

We assume liquid water at low temperatures to be a mixture of two interconvertible states or structures, a high-density state A

^{a)} Author to whom correspondence should be addressed. Electronic mail: anisimov@umd.edu

and a low-density state B. The fraction of molecules in state B is denoted by x , and is controlled by the ‘reaction’



The states A and B could correspond to different arrangements of the hydrogen-bonded network.²² In water-like atomistic models, such as the mW model, these states could correspond to two kinds of local coordination of the water molecules.²³

In a real liquid, molecular configurations form a continuous distribution of coordination numbers and local structures. Therefore, for real water the division of molecular configurations into two states seems a gross simplification. However, such an approach could serve as a first approximation if the distribution can be decomposed in two populations with distinct properties. A similar concept, “quasi-binary approximation,” is commonly used to describe the properties of multi-component fluids.²⁴ As for any phenomenological model, the utility of the two-state approximation is to be provided by a comparison with experimental or computational data.

Two-state equations of state have become popular to explain liquid polyamorphism.^{25–28} Ponyatovsky *et al.*²⁹ and Moynihan³⁰ assumed that water could be considered as a ‘regular binary solution’ of two states, which implies that the phase separation is driven by energy, and they qualitatively reproduced the thermodynamic anomalies of water. Cuthbertson and Poole³¹ showed that the ST2 water model can be described by a regular-solution two-state equation. Bertrand and Anisimov²¹ introduced a two-state equation of state where water is assumed to be an athermal solution, which undergoes phase separation driven by non-ideal entropy upon increase of the pressure. This equation of state was used by Holten and Anisimov¹⁵ to successfully describe the properties of real supercooled water.

In general, the molar Gibbs energy of a two-state mixture is

$$G = G^A + xG^{BA} + RT[x \ln x + (1-x) \ln(1-x)] + G^E, \quad (2)$$

where R is the gas constant, T is the temperature, $G^{BA} \equiv G^B - G^A$ is the difference in molar Gibbs energy between pure configurations A and B, and G^E is the excess Gibbs energy of mixing. The difference G^{BA} is related to the equilibrium constant K of “reaction” (1) as

$$\ln K(T, P) = \frac{G^{BA}}{RT}, \quad (3)$$

where P is the pressure. For the application to the mW model, we adopt a linear expression for $\ln K$ as the simplest approximation.

$$\ln K = \lambda(\Delta\hat{T} + a\hat{P}), \quad (4)$$

with

$$\Delta\hat{T} = (T - T_0)/T_0, \quad \hat{P} = P/\rho_0 RT_0, \quad (5)$$

where T_0 is the temperature at which $\ln K = 0$ for zero pressure, and ρ_0 is a reference density. The parameter a is proportional to the slope of the $\ln K = 0$ line in the T – P phase

diagram. The parameter λ is proportional to the heat of reaction (1), while the product $v = \lambda a$ is proportional to the volume change of the reaction.

The excess Gibbs energy,

$$G^E = H^E - TS^E, \quad (6)$$

causes the non-ideality of the mixture and is the sum of contributions of the enthalpy of mixing H^E and excess entropy S^E .

The Gibbs energy G^A of the pure structure A defines the background of the properties and is approximated as

$$G^A = RT_0 \sum_{m,n} c_{mn} (\Delta\hat{T})^m \hat{P}^n, \quad (7)$$

where m and n are integers and c_{mn} are adjustable coefficients.

Regular solution

In the case of a regular solution, the non-ideality is entirely associated with the enthalpy of mixing. Taking $H^E = wx(1-x)$, we obtain

$$G = G^A + xG^{BA} + RT[x \ln x + (1-x) \ln(1-x)] + wx(1-x). \quad (8)$$

The interaction parameter w is assumed to be independent of temperature, but may depend on pressure. Considering x , the fraction of B, as the reaction coordinate or extent of reaction,³² the condition of chemical reaction equilibrium,

$$\left(\frac{\partial G}{\partial x} \right)_{T,P} = 0, \quad (9)$$

defines the equilibrium fraction x_e through

$$\ln K + \ln \frac{x_e}{1-x_e} + \frac{w}{RT} (1-2x_e) = 0. \quad (10)$$

If the excess Gibbs energy becomes large enough, phase separation may occur, and a critical point may exist in the phase diagram. In the case of a regular solution, Eq. (8), the conditions for the critical point of liquid–liquid equilibrium,

$$\left(\frac{\partial^2 G}{\partial x^2} \right)_{T,P} = 0, \quad \left(\frac{\partial^3 G}{\partial x^3} \right)_{T,P} = 0, \quad (11)$$

yield the critical composition $x_c = 1/2$ and the condition

$$T = \frac{w(P)}{2R}. \quad (12)$$

If the line in the phase diagram given by Eq. (12) intersects the line given by the phase equilibrium condition $\ln K(T, P) = 0$, a critical point exists at the intersection and a line of liquid–liquid phase equilibrium emanates from this point toward lower temperature. This is an energy-driven phase transition, like in the lattice-gas model.

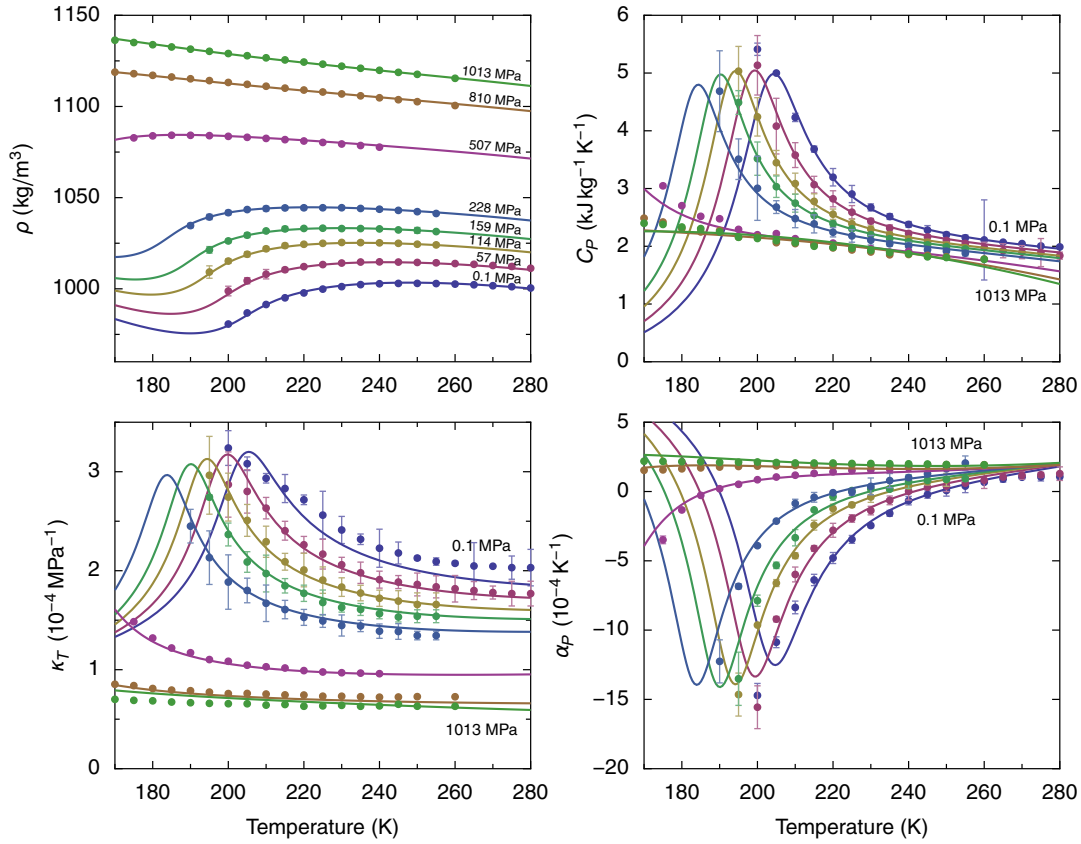


FIG. 1. Density ρ , isobaric heat capacity C_p , isothermal compressibility κ_T , and thermal expansivity α_p computed from the mW model (points) compared with the results (curves) of the two-state approach for an athermal solution [Eq. (13)]. The isobar pressures are given in the density diagram; pressures and corresponding isobar colors are the same for the other plots.

Athermal solution

In the case of an athermal solution, the enthalpy of mixing is zero and the non-ideality is associated with the excess entropy of mixing. With the simplest symmetric form of excess entropy, $S^E = -R\omega x(1-x)$, we obtain

$$G = G^A + xG^{BA} + RT[x \ln x + (1-x) \ln(1-x) + \omega x(1-x)]. \quad (13)$$

The equilibrium fraction x_e is given by

$$\ln K + \ln \frac{x_e}{1-x_e} + \omega(1-2x_e) = 0. \quad (14)$$

The critical-point conditions of Eq. (11) yield the critical value

$$\omega_c = 2. \quad (15)$$

Thus, the critical pressure P_c is the pressure at which the function $\omega(P)$ reaches the value 2. The critical temperature T_c follows from the phase-equilibrium condition, $\ln K(T_c, P_c) = 0$. If the function $\omega(P)$ remains below 2 for all pressures, a critical point does not exist and the mixture does not phase separate. If ω is larger than 2 for a certain pressure, an entropy-driven phase transition exists. While real water shows a preference for the athermal two-state description,¹⁵ the experimental data cannot exclude a contribution of energy in the non-ideal part of the Gibbs energy.

Clustering of water molecules

Moore and Molinero²³ have demonstrated that four-coordinated molecules cluster in supercooled mW water, an idea originally proposed by Stanley and Teixeira.³³ The formation of clusters of molecules belonging to a single state reduces the number of configurations and decreases the mixing entropy. Clustering can be incorporated in the equation of state by dividing the ideal mixing entropy terms by the number of molecules in a cluster N . For the athermal solution, Eq. (13), this yields

$$G = G^A + xG^{BA} + RT \left[\frac{x}{N_1} \ln x + \frac{1-x}{N_2} \ln(1-x) + \omega x(1-x) \right]. \quad (16)$$

Formally, this expression is identical to the free energy of a mixture of two polymers with (large) degrees of polymerization N_1 and N_2 in Flory–Huggins theory.³⁴ However, in our case these parameters are purely phenomenological. In principle, the cluster sizes N_1 and N_2 are functions of temperature and pressure. In this work, we use a constant $N_1 = N_2 = N$ as a first approximation. Furthermore, one can imagine a mixed scenario in which the system combines both athermal-solution and regular-solution features.

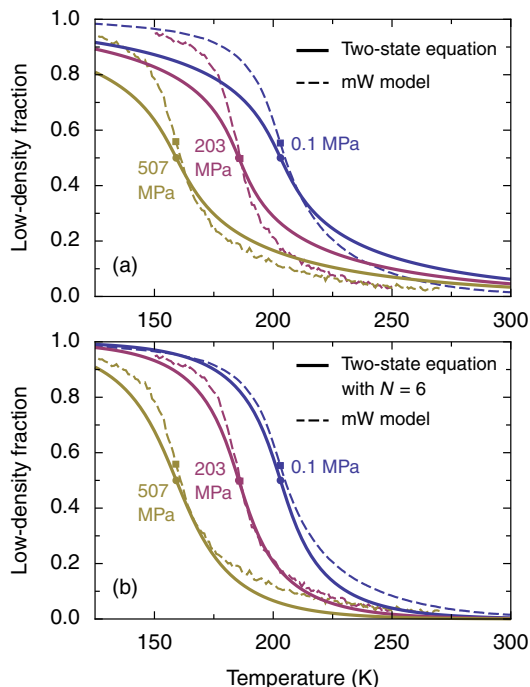


FIG. 2. Fraction x of molecules in the low-density state, Solid curves: fraction x for the (a) two-state equation of state, Eq. (13); (b) two-state equation with account for hexamer clustering, Eq. (16) with $N = 6$. Dashed curves: fraction x obtained from simulations of mW water, calculated from the fraction of four-coordinated molecules f_4 as $x = (f_4 - f_4^H)/(f_4^L - f_4^H)$, to account for fractions f_4^L and f_4^H of four-coordinated molecules in the low- and high-temperature liquid, respectively. The inflection points on the curves are marked with circles (two-state equation) and squares (mW model). The data was collected by linearly quenching the temperature of the simulations at a rate of 10 K/ns. The data below the inflection point do not correspond to equilibrium states.

Description of thermodynamic properties of the mW model

Thermodynamic properties of the mW model, namely density, isothermal compressibility, and heat capacity have been calculated from molecular dynamics simulations by Limmer and Chandler up to 228 MPa.²⁰ For this work, the expansion coefficient has also been calculated, and the calculations have been extended to higher pressures, as shown in Fig. 1. We apply the two-state thermodynamics of water to explain and reproduce the calculated properties and demonstrate that this model does not show liquid–liquid separation, at least in the range of pressures and temperatures studied.

First, we have verified whether an “ideal-solution” two-state thermodynamics, for which the excess Gibbs energy is zero, can reproduce the thermodynamic properties of the mW model. Indeed, the competition between these two states, even without non-ideality, can cause the density maximum and the increase in the response functions. However, the thermodynamic properties are not the only data that should be matched. Moore and Molinero²³ have calculated the fraction of four-coordinated molecules f_4 , which is a fraction of molecules in a low-density state (Fig. 2). Specifically, f_4 is the fraction

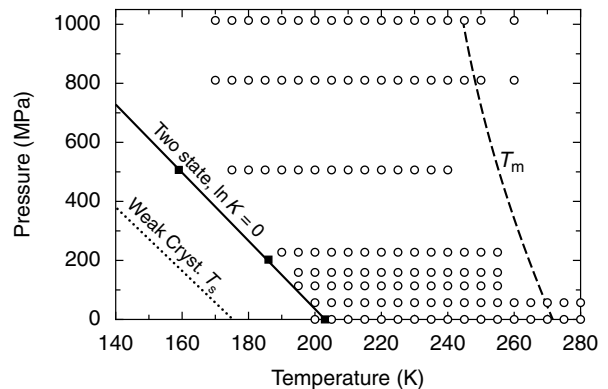


FIG. 3. Pressure–temperature diagram. Circles: location of the computed property data of the mW model. Solid line: line at which $\ln K = 0$ and the low-density fraction $x = 1/2$ for the two-state equation. Squares: location of inflection points of the low-density fraction x for the mW model (see Fig. 2). Dotted line: stability-limit temperature T_s from the fit of the weak crystallization model to the mW data, Eq. (26). The dashed curve is a fit to the melting temperature T_m of mW ice (uncertainty about ± 3 K), obtained from free energy calculations as described in Ref. 20.

of molecules with four neighbors within the first coordination shell up to a certain cutoff radius r_c . The exact value of f_4 depends on the value of r_c , but the inflection point of the $f_4(T)$ curve is independent of r_c and occurs at $T_i = (201 \pm 2)$ K at atmospheric pressure.²³ The value of r_c was 0.35 nm for all pressures in this study. This cutoff corresponds to the first solvation shell, as the position of the first minimum of the radial distribution function of mW water is 0.35 nm at 0.1 MPa and 0.342 nm at 507 MPa. The fraction x of low-density liquid is related to f_4 by

$$x(T) = \frac{f_4(T) - f_4^H}{f_4^L - f_4^H}, \quad (17)$$

which accounts for the finite fraction f_4^H of four-coordinated molecules in the high-temperature liquid, and the fraction $f_4^L < 1$ of four-coordinated molecules in the low-temperature liquid. Both f_4^H and f_4^L are estimated by an extrapolation of the fraction f_4 to high and low temperature. Below T_i , liquid mW water cannot be equilibrated without crystallization.¹⁹ Nevertheless, the fraction f_4 was also computed below T_i as in Ref. 23: in quenching simulations the temperature was varied linearly at 10 K/ns, the slowest rate that results in the vitrification of mW water. Liquid mW water can be equilibrated down to T_i at a cooling rate of 10 K/ns, but any property extracted from the quenching simulations at $T < T_i$ may depend on the cooling rate.

In the two-state thermodynamics, as given by Eq. (10) or Eq. (14), the inflection point of the fraction x at atmospheric pressure occurs where $\ln K = 0$, near the temperature T_0 [Eq. (5)]. To match the low-density fraction of the mW model, T_0 should be close to T_i . This is not the case for the ideal-solution two-state version, where $T_0 = (160 \pm 4)$ K, significantly below T_i .

With a nonzero excess Gibbs energy, the two-state approach is able to reproduce both the thermodynamic properties and

the inflection point of the fraction in the mW model. As Fig. 3 shows, the inflection points of the fraction of low-density liquid in mW simulations at different pressures form a straight line in the phase diagram. Since the two-state equation yields inflection points at the line $\ln K = 0$, the inflection points of the mW model can be matched by adopting suitable values of the slope a and intercept T_0 of the $\ln K = 0$ line [Eq. (4)]. When the $\ln K = 0$ line is fixed in this way, the athermal-solution (entropy-driven non-ideality) version yields a better description than the regular-solution (energy-driven non-ideality) version; the sum of squared deviations of the regular-solution fit from the thermodynamic property data is about 50% higher than that of the athermal-solution fit. More convincing evidence in favor of the athermal-solution approximation comes from the direct computation of the enthalpy and entropy of mW water; see below. An approximation with a constant interaction parameter, w or ω , works reasonably well, and the description can be further improved by making the interaction parameter weakly dependent on pressure. In the case of the athermal-solution version, the two-state thermodynamics for the mW model excludes liquid–liquid separation at any temperature or pressure, because the value of ω is lower than 2 (for a pressure-independent ω , the optimum value is 1.61). In the case of the regular-solution version, the two-state thermodynamics for the mW model predicts liquid–liquid separation at a temperature below 147 K, which is outside the kinetic limit of metastability of mW liquid water.¹⁹ Figure 1 shows the predicted thermodynamic properties for the athermal-solution case with a quadratic pressure dependence of ω , and Fig. 2a shows the low-density fraction. The numerical values of all parameters are given in the appendix. At 0.1 MPa, there is a systematic difference between compressibility values calculated from the two-state equation and those of the mW model. This difference can be decreased by including more background terms, but that would make the description more empirical.

An improved description of the low-density fraction is obtained when clustering of water molecules is taken into account in the equation of state, as in Eq. (16). When the number of molecules N in a cluster is taken as an adjustable parameter in the fit, the optimum value is 6.5, but the quality of the fit varies little for values of N between 4 and 10. For clusters of $N = 6$ molecules (hexamers), the fraction that results from the fit to the mW properties is shown in Fig. 2b. Because of the division of the ideal mixing entropy terms by N in Eq. (16), a smaller non-ideality term is sufficient. Indeed, for the fit with $N = 6$, the value of the interaction parameter ω is 0.2, an order of magnitude smaller than in the case without cluster formation. For such a small value of ω , the difference between a regular and an athermal solution becomes unimportant, because the main contribution to the nonideality comes from clustering and thus is entropy driven. The work of Moore and Molinero²³ shows that clustering of four-coordinated molecules increases with cooling, which suggests that the parameter N_1 is temperature dependent. Such a temperature-dependent N_1 would affect the values of the properties calculated with the two-state thermodynamics, particularly at low temperature.

Analysis of the enthalpy of liquid water supports the con-

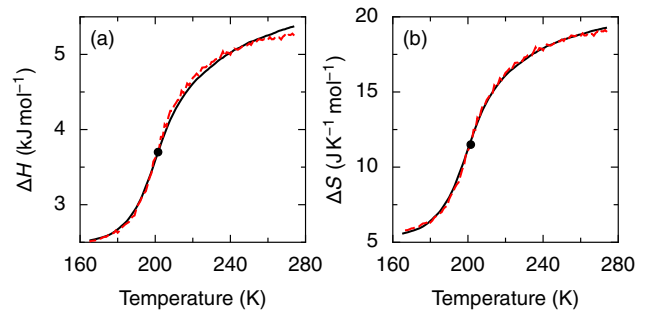


FIG. 4. Enthalpy ΔH (a) and entropy ΔS (b) of liquid mW water with respect to ice at 0.1 MPa (black curves, from Moore and Molinero¹⁹) and their fits (dashed) according to Eqs. (18) and (19), respectively. Both ΔH and ΔS are computed at a cooling rate of 10 K/ns, which prevents crystallization, so that the values below 200 K do not correspond to an equilibrium state. The circle signals $T_i = 201$ K. These results support the modeling of mW water as an athermal mixture of two states.

jecture that the excess free energy of mixing is almost entirely due to entropic effects. If water is represented as a “mixture,” then its enthalpy can be written in terms of the partial molar enthalpies of the low and high-density “components”. Figure 4 shows that the enthalpy of liquid water with respect to ice in mW water is very well represented by a sum of the weighted contributions of the two pure components, i.e., no excess enthalpy of mixing:

$$\Delta H = H_{\text{liq}} - H_{\text{ice}} = [1.84x + 5.38(1 - x)] \text{ kJ/mol}. \quad (18)$$

Here we use the enthalpy with respect to ice, instead of the enthalpy itself, to eliminate the trivial temperature dependence of the partial molar enthalpies of the components. This is possible in mW water because the heat capacity of the four-coordinated component is almost indistinguishable from that of mW ice, and the heat capacity of the high-temperature component is also quite close to that of ice, as a result of the monatomic nature of the model. Thus, the temperature dependence of the molar enthalpy difference between a component and ice is negligible.

The enthalpy of the low-density component with respect to ice, 1.84 kJ/mol, is in good agreement with the (1.35 ± 0.15) kJ/mol measured for LDA in experiments.³⁵ The enthalpy of the high-density component with respect to ice is, unsurprisingly, the enthalpy of melting of ice (5.3 kJ/mol for mW, 6.0 kJ/mol in experiments). These results support the interpretation that there is no excess enthalpy of mixing contribution to the non-ideal excess free energy of liquid mW water.

Interestingly, the entropy of liquid water with respect to ice can also be represented as a weighted sum of temperature-independent contributions from the two pure components (Fig. 4):

$$\Delta S = S_{\text{liq}} - S_{\text{ice}} = [2.18x + 19.75(1 - x)] \text{ J/(K mol)}, \quad (19)$$

where the entropy of the low-density component with respect to ice, 2.18 J/(K mol), is in good agreement with the experimental value for LDA, (1.6 ± 1.0) J/(K mol),³⁶ and the entropy of the high-density component with respect to ice is the

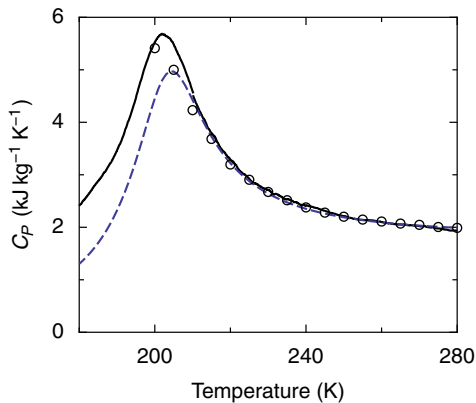


FIG. 5. Heat capacity of mW water in equilibrium (circles) and on hyperquenching at 10 K/ns (black curve, computations by Moore and Molinero¹⁹). The values below 200 K do not correspond to an equilibrium state. The dashed curve is the prediction of the two-state equation with hexamer clusters.

entropy of melting (19.3 J/(K mol) for mW water, 22 J/(K mol) in experiment). The implication of Eq. (19) is that mW water is an “athermal solution,” the excess (non-ideal) entropy of mixing is negative, and – remarkably – it essentially cancels out the positive ideal entropy of mixing contribution. This cancellation strongly supports the idea of molecular clustering and is similar to the thermodynamics of near-athermal mixtures of two high-molecular-weight polymers, where the entropy of mixing is very small. This property of mW water excludes the possibility of the regular-solution approximation.

Figure 5 shows the isobaric heat capacity C_P calculated for liquid mW water down to a temperature below the crystallization temperature, which is made possible by hyperquenching at 10 K/ns. Below 200 K, the two-state thermodynamics predicts a C_P that is lower than the value for hyperquenched mW water. This discrepancy may be caused by an oversimplicity of our equation of state, in particular the symmetric form of the excess entropy of mixing $S^E = -R\omega x(1-x)$ and the constant value of N .

The two-state thermodynamics predicts maxima of the heat capacity and compressibility, and minima of the density and expansivity near the line $\ln K = 0$. These extrema are not observed in simulations of the equilibrium mW liquid, shown in Fig. 1, but they are seen when the system is driven out of equilibrium through fast cooling rates, as in Fig. 5. Furthermore, the two-state thermodynamics cannot predict the stability limit of the liquid phase or account for any pre-crystallization effects.

III. WEAK CRYSTALLIZATION THEORY

According to the theory of weak crystallization,^{37–39} fluctuations of the translational order parameter cause corrections in the thermodynamic response functions close to the absolute stability limit of the liquid phase with respect to crystalliza-

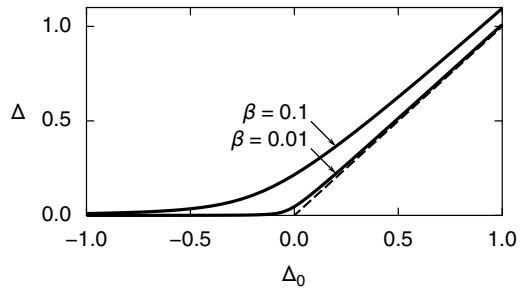


FIG. 6. Fluctuation-renormalized distance to the stability-limit temperature Δ , given by Eq. (21), as a function of the mean-field distance to the stability limit Δ_0 , for two values of β (solid curves). The dashed line corresponds to $\Delta = \Delta_0$ and is shown as a reference.

tion. The distance to the stability limit Δ is defined as

$$\Delta(T, P) = \frac{T - T_s(P)}{T_s(P)}, \quad (20)$$

where T is the temperature, P is the pressure, and $T_s(P)$ is the stability-limit temperature. According to this theory, the fluctuations of the translational (short-wavelength) order parameter ψ renormalize the mean-field distance $\Delta_0 = (T - T_s^{\text{MF}})/T_s^{\text{MF}}$ between the temperature T and the mean-field absolute stability limit T_s^{MF} of the liquid phase:

$$\Delta = \Delta_0 + \beta \Delta^{-1/2}, \quad (21)$$

where Δ is the fluctuation-renormalized distance to the stability-limit temperature, and β is a molecular parameter, similar to the Ginzburg number that defines the validity of the mean-field approximation in the theory of critical phenomena. Solutions of Eq. (21) are shown in Fig. 6. Fluctuations of the translational order parameter stabilize the liquid phase, shifting the stability limit of the liquid below the mean-field value, meaning that Δ_0 becomes negative at Δ tending to zero. This also means that the fluctuation part would not actually diverge. Thus the theory of weak crystallization requires $\beta \Delta^{-1/2} \ll \Delta_0$ and $\Delta_0 \ll 1$. As seen in Fig. 6, even the value of the coupling constant $\beta = 0.1$ is already beyond the validity limit of the theory since it corresponds to the mean-field gap $\Delta_0 = -1$.

The contribution of order-parameter fluctuations to the isobaric heat capacity C_P and isothermal compressibility κ_T is proportional to $\Delta^{-3/2}$, while the contribution to the density and entropy is $\sim \Delta^{-1/2}$. Accordingly, the fluctuation contribution $\delta \hat{\mu} = \hat{\beta} \Delta^{1/2}$ can be included in the chemical potential $\hat{\mu}$ as

$$\hat{\mu} = \hat{\beta} \Delta^{1/2} + \hat{\mu}^r(\hat{T}, \hat{P}), \quad (22)$$

where $\hat{\beta} \simeq 2\beta$ (see the appendix) is the amplitude of the fluctuation part, and $\hat{\mu}^r$ is the regular (background) part of the chemical potential. The contributions from fluctuations are to be small compared to the background. The variables with a hat in Eq. (22) are dimensionless variables, defined as

$$\hat{T} = \frac{T}{T_{s0}}, \quad \hat{\mu} = \frac{\mu}{RT_{s0}}, \quad \hat{P} = \frac{PV_0}{RT_{s0}}, \quad (23)$$

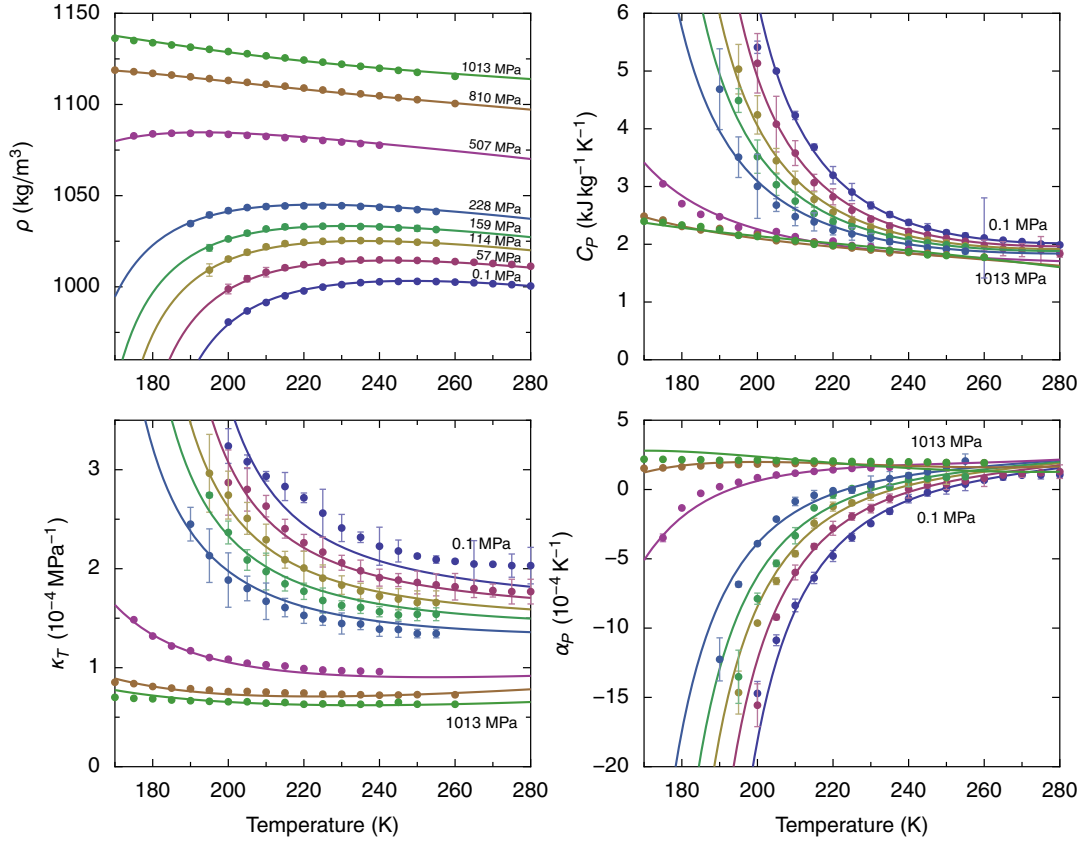


FIG. 7. Density ρ , isobaric heat capacity C_p , isothermal compressibility κ_T , and thermal expansivity α_p computed from the mW model (points) compared with the fit to power laws given by weak crystallization theory (curves). The isobar pressures are given in the density diagram; pressures and corresponding isobar colors are the same for the other plots.

where T_{s0} is the stability-limit temperature at zero pressure, R is the molar gas constant, and $V_0 = M \times 10^{-3} \text{ m}^3/\text{kg}$ is an arbitrary reference constant for the molar volume, with M the molar mass of water. For our application of the weak crystallization theory to the mW model results, we represent the regular part $\hat{\mu}^r$ by a truncated Taylor-series expansion,

$$\hat{\mu}^r(\hat{T}, \hat{P}) = \sum_{m,n} c_{mn} \hat{T}^m \hat{P}^n, \quad (24)$$

similar to Eq. (7). We approximate the dependence of the stability-limit temperature on the pressure by a linear function,

$$\hat{T}_s(\hat{P}) = 1 - d' \hat{P}, \quad (25)$$

where the slope d' is an adjustable parameter. Expressions for the thermodynamic properties, found from derivatives of the chemical potential of Eq. (22), are given in the appendix.

Fit to the mW data

A fit of Eq. (22) to the mW data, shown in Fig. 7, results in a stability-limit temperature of

$$T_s(P)/K = 175 - 0.093(P/\text{MPa}), \quad (26)$$

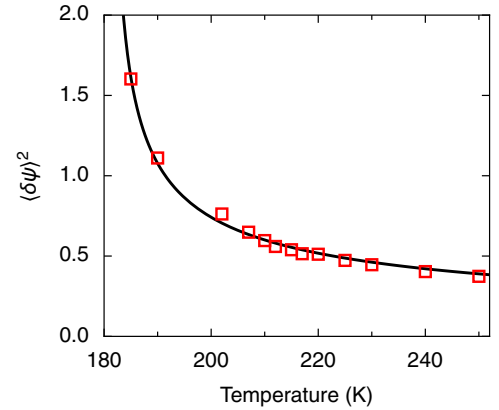


FIG. 8. Fluctuations of the crystallization order parameter from weak crystallization theory (i.e. short-wavelength density fluctuations) in arbitrary units as a function of temperature, fit with Eq. (28) (curve).

which is shown in Fig. 3, and an amplitude of⁴⁰

$$\hat{\beta} = 2.3 \pm 0.4. \quad (27)$$

As shown in the appendix, the amplitude $\hat{\beta}$ is related to the coupling constant β as $\hat{\beta} \simeq 2\beta$. To verify whether there is a microscopic manifestation of weak crystallization theory,

we have computed the normalized short-wavelength density fluctuations, corresponding to the fluctuations of the order parameter ψ from weak crystallization theory, at atmospheric pressure as a function of temperature. The quantity plotted in Fig. 8 is dimensionless but its magnitude is not defined unambiguously. It is calculated by taking the expectation value over the Fourier transform of the density operator which results in the form $\langle \exp(iqr) \exp(-iqr) \rangle$ where r is a particle position and q is the wavenumber. The wavenumber is chosen at the highest peak in the structure factor. The computation is performed for an $N = 8000$ particle system at a constant pressure of 0.1 MPa, and each point is averaged over 10 ns. The fluctuations would diverge in the thermodynamic limit for a crystal, illustrating the broken symmetry. In the liquid phase, the order parameter $\langle \psi \rangle = 0$. Figure 8 shows the order parameter fluctuations together with a fit of the form

$$\langle \delta\psi \rangle^2 = b[(T - T_s)/T_s]^{-1/2}, \quad (28)$$

where b is a constant proportional to the coupling constant β in Eq. (21). From the fit we obtain $b \simeq 0.24$ and $T_s \simeq 181$ K, close to the value of 175 K found above. Another way to estimate T_s is by extrapolating the surface tension between liquid and crystal as a function of supercooling, and finding the temperature at which it becomes zero. An extrapolation of the surface tension values of Limmer and Chandler⁴¹ yields $T_s \simeq 170$ K. The stability-limit temperature T_s lies far below the temperature of maximum crystallization rate determined by Moore and Molinero,¹⁹ which is 202 K at 0.1 MPa and signals the lowest temperature at which liquid mW water can be equilibrated. This temperature difference should not be interpreted as a disagreement, because the temperature of maximum crystal growth is a kinetic quantity and does not correspond to a thermodynamic instability.

While the weak crystallization model provides a reasonable description of the mW data as shown in Fig. 7, the amplitude $\hat{\beta} \simeq 2\beta \simeq 2$ is not small compared to unity, contradicting Eq. (21), which is based on the assumption of small fluctuation corrections in the theory. The fit based on weak crystallization theory also implies that the density maximum at atmospheric pressure is caused by translational short-wavelength fluctuations of density. This is unphysical because such fluctuations should not have a significant effect far (100 K) from the stability limit of the liquid state, where the density maximum is observed. Moreover, weak crystallization theory predicts universal fluctuation-induced corrections to the regular behavior of thermodynamic properties and is equally applicable to all metastable fluids, not only to tetrahedral fluids that expand on freezing and exhibit a density maximum.

That the weak-crystallization power laws provide a good empirical description of water's anomalies is not surprising. The properties of real supercooled water can also be described quite well with purely empirical power laws diverging along a certain line below the homogenous ice nucleation limit.^{4,42} The fitted line of apparent singularities and the fitted values of the exponents are strongly correlated and cannot be obtained independently. The larger the exponent value, the further away from the homogenous nucleation this line is shifted.

Adjustable amplitudes of the power laws would increase the ambiguity even further.

However, we cannot ignore the fact that the fluctuations of the crystallization order parameter indeed increase upon supercooling, as demonstrated in Fig. 8. While the relation between the amplitude of this effect and the coupling constant β of weak crystallization theory is unclear, it seems quite plausible that the fluctuations also contribute to the thermodynamic anomalies.

IV. CONCLUSIONS

By fitting properties with equations of state based on different underlying assumptions, the consistency of such assumptions with thermodynamics can be tested. In this way we have examined the origin of the anomalous behavior of the mW model in terms of a two-state model and a model based on weak crystallization.

We have reproduced the anomalies of the mW model with a phenomenology based on a non-ideal mixture of two different molecular configurations in liquid water. While an ideal mixture of these states also generates enhancements in the response functions, agreement with the mW data on the low-density fraction unambiguously requires a non-ideal mixture. However, the nonideality is not strong enough to cause liquid-liquid phase separation in the mW model, in the wide range of pressures and temperatures of this study. An entropy-driven, athermal-solution-like nonideality gives a better description of the mW data than an energy-driven, regular-solution-like nonideality. Incorporating the formation of clusters into the equation of state results in a further improvement of the description of the low-density fraction in mW water. The thermodynamic treatment of the two-state model used here is independent of the details of the states considered. Microscopically, however, there is no unique projection for defining these states from the continuum distribution of configurations.

A description which uses the power laws of weak crystallization theory succeeds in reproducing the calculated mW properties. The required-by-fit value of the coupling constant appears to be about 2, which contradicts the assumption of the theory where this constant is essentially a small parameter. Finally, weak crystallization theory is based on the existence of the liquid-state stability limit and accounts for the growing short-wave density fluctuations near that limit, which indeed are found in simulations.^{19,20} However, unlike the two-state approach, it cannot account for the data on the fraction of four-coordinated molecules. The need to consider fluctuation effects due to crystallization is consistent with previous work on the modulation of ice interfaces in real water.⁴¹ This previous work demonstrated that such fluctuations are important in describing how crystallization is altered in confinement and suggests that such effects can be correctly accounted for within simple Gaussian corrections. Reconciling the anomalous thermodynamics that are well recovered by the two-state model, with the unavoidable effects of crystallization is an important avenue to pursue in the future.

ACKNOWLEDGMENTS

The authors have benefited from numerous interactions with Pablo Debenedetti (Princeton University). Jan V. Sengers (University of Maryland, College Park) read the manuscript and made useful comments. M.A.A. acknowledges discussions with Efim I. Kats (Landau Institute, Russia) on weak crystallization theory. The research of V.H. and M.A.A. has been supported by the Division of Chemistry of the U.S. National Science Foundation under Grant No. CHE-1012052. D.T.L. acknowledges the Helios Solar Energy Research Center, which is supported by the Director, Office of Science, Office of Basic Energy Sciences of the U.S. Department of Energy under Contract No. DE-AC02-05CH11231. V.M. acknowledges support by the National Science Foundation through awards CHE-1012651 and CHE-1125235 and the Camille and Henry Dreyfus Foundation through a Teacher-Scholar Award.

APPENDIX

Expressions for thermodynamic properties in weak crystallization theory

From derivatives of the chemical potential of Eq. (22), we obtain

$$\hat{V} = \left(\frac{\partial \hat{\mu}}{\partial \hat{P}} \right)_T = \frac{\hat{\beta} a' \hat{T}}{2 \hat{T}_s^2 \Delta^{1/2}} + \hat{\mu}_{\hat{P}}^r, \quad (29)$$

$$\hat{S} = - \left(\frac{\partial \hat{\mu}}{\partial \hat{T}} \right)_P = - \frac{\hat{\beta}}{2 \hat{T}_s \Delta^{1/2}} - \hat{\mu}_{\hat{T}}^r, \quad (30)$$

$$\hat{C}_P = \hat{T} \left(\frac{\partial \hat{S}}{\partial \hat{T}} \right)_P = \hat{T} \left(\frac{\hat{\beta}}{4 \hat{T}_s^2 \Delta^{3/2}} - \hat{\mu}_{\hat{T}\hat{T}}^r \right), \quad (31)$$

$$\hat{\kappa}_T = - \frac{1}{\hat{V}} \left(\frac{\partial \hat{V}}{\partial \hat{P}} \right)_T = \frac{1}{\hat{V}} \left(\frac{\hat{\beta} a'^2 \hat{T}^2}{4 \hat{T}_s^4 \Delta^{3/2}} - \frac{\hat{\beta} a'^2 \hat{T}}{\hat{T}_s^3 \Delta^{1/2}} - \hat{\mu}_{\hat{P}\hat{P}}^r \right), \quad (32)$$

$$\hat{\alpha}_P = \frac{1}{\hat{V}} \left(\frac{\partial \hat{V}}{\partial \hat{T}} \right)_P = \frac{1}{\hat{V}} \left(- \frac{\hat{\beta} a' \hat{T}}{4 \hat{T}_s^3 \Delta^{3/2}} + \frac{\hat{\beta} a'}{2 \hat{T}_s^2 \Delta^{1/2}} + \hat{\mu}_{\hat{T}\hat{P}}^r \right). \quad (33)$$

where $\hat{V} = V/V_0$, \hat{S} , \hat{C}_P , $\hat{\kappa}_T$ and $\hat{\alpha}_P$ are the dimensionless volume, entropy, isobaric heat capacity, isothermal compressibility and the thermal expansivity, respectively. The subscripts of $\hat{\mu}^r$ indicate a partial derivative of $\hat{\mu}^r$ with respect to the subscripted quantities.

Relation between the amplitude $\hat{\beta}$ and the coupling constant β in weak crystallization theory

Consider the temperature-squared term in the dimensionless chemical potential $\hat{\mu}$,

$$c \hat{T}^2 = c \hat{T}_s^2 (\Delta + 1)^2 = c \hat{T}_s^2 (\Delta^2 + 2\Delta + 1). \quad (34)$$

TABLE I. Parameters for the two-state equation of state, Eq. (13)

| Parameter | Value | Parameter | Value |
|-------------|---------------------------|-----------|--------------------------|
| T_0 | 203.07 K | c_{03} | 1.5125×10^{-4} |
| ρ_0 | 1000.0 kg m ⁻³ | c_{05} | -1.5795×10^{-7} |
| λ | 2.6917 | c_{11} | 8.4408×10^{-2} |
| ω_0 | 1.6362 | c_{12} | -3.9163×10^{-3} |
| ω_1 | 1.6777 | c_{13} | 1.2385×10^{-4} |
| \hat{P}_1 | 2.3219 | c_{20} | -1.7092×10^0 |
| a | 0.039968 | c_{21} | -4.3879×10^{-2} |
| c_{01} | 9.5440×10^{-1} | c_{30} | 4.0687×10^{-1} |
| c_{02} | -5.0517×10^{-3} | c_{31} | 6.1937×10^{-2} |

$$\chi^2 = 0.82$$

TABLE II. Parameters for the two-state equation, Eq. (16), with $N = 6$

| Parameter | Value | Parameter | Value |
|-------------|---------------------------|-----------|--------------------------|
| T_0 | 203.07 | c_{03} | 2.8467×10^{-4} |
| ρ_0 | 1000.0 kg m ⁻³ | c_{05} | -3.1836×10^{-7} |
| λ | 1.529 | c_{11} | 3.9710×10^{-2} |
| ω_0 | 0.19523 | c_{12} | -6.4543×10^{-4} |
| ω_1 | 0.19856 | c_{13} | 4.6055×10^{-5} |
| \hat{P}_1 | 1.1637 | c_{20} | -1.8630×10^0 |
| a | 0.039968 | c_{21} | -3.2135×10^{-2} |
| c_{01} | 9.8530×10^{-1} | c_{30} | 3.3420×10^{-1} |
| c_{02} | -8.1978×10^{-3} | c_{31} | 5.7351×10^{-2} |

$$\chi^2 = 0.72$$

Considering the Δ^2 term, using Eq. (21) gives

$$\begin{aligned} \Delta^2 &= \Delta_0^2 + 2\beta \Delta_0 \Delta^{-1/2} + \beta^2 \Delta^{-1} \\ &= \Delta_0^2 + 2\beta \Delta^{1/2} - \beta^2 \Delta^{-1}. \end{aligned} \quad (35)$$

The last term can be neglected because according to the theory $\beta \ll 1$. Since this is not the case in our attempt to apply weak crystallization theory to the mW data, such a description becomes purely empirical.

The first term on the right-hand side Δ_0^2 is part of the regular part of the chemical potential, and the second term $2\beta \Delta^{1/2}$ leads to the fluctuation contribution $\delta \hat{\mu}$ in the chemical potential of

$$\delta \hat{\mu} = 2c \hat{T}_s^2 \beta \Delta^{1/2}. \quad (36)$$

Comparing this with Eq. (22) gives the relation between $\hat{\beta}$ and β ,

$$\hat{\beta} = 2c \hat{T}_s^2 \beta. \quad (37)$$

For our fit to the mW data, $c \simeq 1$ and $\hat{T}_s \simeq 1$, so Eq. (37) gives

$$\hat{\beta} \simeq 2\beta. \quad (38)$$

Parameter values

Parameters for the two-state equation of state, Eq. (13), are listed in Table I, and those for the fit of the equation with clusters of six molecules, Eq. (16), are given in Table II. The value

TABLE III. Parameters for the fit of weak crystallization theory, Eq. (22)

| Parameter | Value | Parameter | Value |
|---------------|----------------------------|-----------|--------------------------|
| T_{s0} | 175.28 K | c_{11} | 4.2389×10^{-1} |
| M/V_0 | 1000.0 kg m^{-3} | c_{12} | -3.3672×10^{-4} |
| $\hat{\beta}$ | 2.3254 | c_{13} | -1.3649×10^{-4} |
| a' | 0.042825 | c_{20} | 3.4178×10^{-1} |
| c_{01} | 6.1915×10^{-1} | c_{21} | -2.3514×10^{-1} |
| c_{02} | -8.2724×10^{-3} | c_{30} | -2.2560×10^{-1} |
| c_{03} | 3.6026×10^{-4} | c_{31} | 4.9163×10^{-2} |
| c_{05} | -6.6486×10^{-7} | | |

$$\chi^2 = 0.72$$

of the interaction parameter ω depends quadratically on the pressure,

$$\omega(\hat{P}) = \omega_1 - (\omega_1 - \omega_0) \left[\frac{(\hat{P} - \hat{P}_1)}{\hat{P}_1} \right]^2, \quad (39)$$

where ω_0 is the value of ω at $\hat{P} = 0$, ω_1 is the maximum value of ω , and \hat{P}_1 is the dimensionless pressure at which the maximum occurs. The parameter values for the fit of weak crystallization theory to the mW data are given in Table III. All tables give χ^2 , the reduced sum of squared deviations of the fit from the data.

- ¹C. A. Angell, M. Oguni, and W. J. Sichina, *J. Phys. Chem.* **86**, 998 (1982).
²D. E. Hare and C. M. Sorensen, *J. Chem. Phys.* **87**, 4840 (1987).
³H. Kanno and C. A. Angell, *J. Chem. Phys.* **73**, 1940 (1980).
⁴H. Kanno and C. A. Angell, *J. Chem. Phys.* **70**, 4008 (1979).
⁵P. H. Poole, F. Sciortino, U. Essmann, and H. E. Stanley, *Nature (London)* **360**, 324 (1992).
⁶O. Mishima and H. E. Stanley, *Nature* **396**, 329 (1998).
⁷H. E. Stanley, S. V. Buldyrev, M. Canpolat, O. Mishima, M. R. Sadr-Lahijany, A. Scala, and F. W. Starr, *Phys. Chem. Chem. Phys.* **2**, 1551 (2000).
⁸P. G. Debenedetti, *J. Phys.: Condens. Matter* **15**, R1669 (2003).
⁹K. Stokely, M. G. Mazza, H. E. Stanley, and G. Franzese, *Proc. Natl. Acad. Sci. U.S.A.* **107**, 1301 (2010).
¹⁰O. Mishima, *Proc. Jpn. Acad., Ser. B* **86**, 165 (2010).

- ¹¹O. Mishima and H. E. Stanley, *Nature* **392**, 164 (1998).
¹²O. Mishima, *Phys. Rev. Lett.* **85**, 334 (2000).
¹³O. Mishima, *J. Phys. Chem. B* **115**, 14064 (2011).
¹⁴K. Murata and H. Tanaka, *Nature Mater.* **11**, 436 (2012).
¹⁵V. Holten and M. A. Anisimov, *Sci. Rep.* **2**, 713 (2012).
¹⁶P. G. Debenedetti, *Metastable Liquids* (Princeton University Press, Princeton, NJ, 1996).
¹⁷H. Kanno, R. J. Speedy, and C. A. Angell, *Science* **189**, 880 (1975).
¹⁸V. Molinero and E. B. Moore, *J. Phys. Chem. B* **113**, 4008 (2009).
¹⁹E. B. Moore and V. Molinero, *Nature* **479**, 506 (2011).
²⁰D. T. Limmer and D. Chandler, *J. Chem. Phys.* **135**, 134503 (2011).
²¹C. E. Bertrand and M. A. Anisimov, *J. Phys. Chem. B* **115**, 14099 (2011).
²²D. Eisenberg and W. Kauzmann, "The structure and properties of water," (Oxford University Press, New York, 1969) pp. 256–267.
²³E. B. Moore and V. Molinero, *J. Chem. Phys.* **130**, 244505 (2009).
²⁴V. Valyashko, ed., *Hydrothermal Properties of Materials: Experimental Data on Aqueous Phase Equilibria and Solution Properties at Elevated Temperatures and Pressures* (Wiley, Chichester, UK, 2008).
²⁵P. F. McMillan, *J. Mater. Chem.* **14**, 1506 (2004).
²⁶M. C. Wilding, M. Wilson, and P. F. McMillan, *Chem. Soc. Rev.* **35**, 964 (2006).
²⁷M. Vedamuthu, S. Singh, and G. W. Robinson, *J. Phys. Chem.* **98**, 2222 (1994).
²⁸H. Tanaka, *Eur. Phys. J. E* **35**, 113 (2012).
²⁹E. G. Ponyatovsky, V. V. Sinitsyn, and T. A. Pozdnyakova, *J. Chem. Phys.* **109**, 2413 (1998).
³⁰C. T. Moynihan, *Mat. Res. Soc. Symp. Proc.* **455**, 411 (1997).
³¹M. J. Cuthbertson and P. H. Poole, *Phys. Rev. Lett.* **106**, 115706 (2011).
³²I. Prigogine and R. Defay, *Chemical Thermodynamics* (Longmans, Green & Co., London, 1954).
³³H. E. Stanley and J. Teixeira, *J. Chem. Phys.* **73**, 3404 (1980).
³⁴P. J. Flory, *Principles of Polymer Chemistry* (Cornell University Press, Ithaca, NY, 1953).
³⁵M. A. Floriano, Y. P. Handa, D. D. Klug, and E. Whalley, *J. Chem. Phys.* **91**, 7187 (1989).
³⁶R. S. Smith, J. Matthiesen, J. Knox, and B. D. Kay, *J. Phys. Chem. A* **115**, 5908 (2011).
³⁷S. A. Brazovskii, *Sov. Phys.–JETP* **41**, 85 (1975).
³⁸S. A. Brazovskii, I. E. Dzyaloshinskiĭ, and A. R. Muratov, *Sov. Phys.–JETP* **66**, 625 (1987).
³⁹E. I. Kats, V. V. Lebedev, and A. R. Muratov, *Phys. Rep.* **228**, 1 (1993).
⁴⁰For values of $\hat{\beta}$ in the given range, the sum of squared deviations of the model from the data varies by 5% or less.
⁴¹D. T. Limmer and D. Chandler, *J. Chem. Phys.* **137**, 044509 (2012).
⁴²R. J. Speedy and C. A. Angell, *J. Chem. Phys.* **65**, 851 (1976).